Volume 52 | Number 99 | 25 December 2016 | Pages 14175–14336

ChemComm

Chemical Communications

www.rsc.org/chemcomm

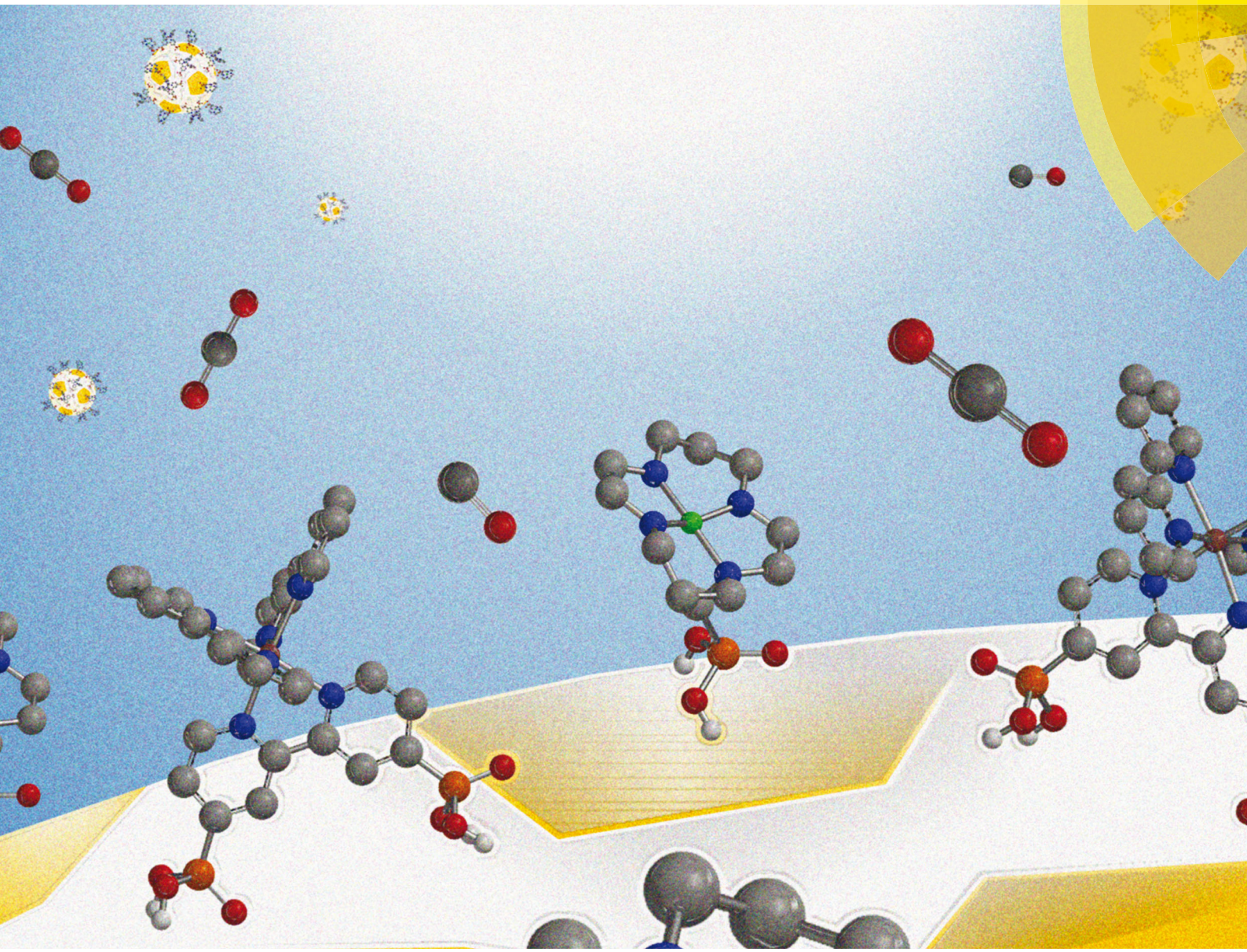

ISSN 1359-7345

ROYAL SOCIETY OF CHEMISTRY

COMMUNICATION

Alexander J. Cowan *et al.*

Photochemical CO_2 reduction in water using a co-immobilised nickel catalyst and a visible light sensitiser

175 YEARS

ChemComm

COMMUNICATION

View Article Online
View Journal | View Issue

Cite this: *Chem. Commun.*, 2016, 52, 14200

Received 25th October 2016,
Accepted 15th November 2016

DOI: 10.1039/c6cc08590c

www.rsc.org/chemcomm

Photochemical CO_2 reduction in water using a co-immobilised nickel catalyst and a visible light sensitiser†

Gaia Neri,[ab] Mark Forster,[ab] James J. Walsh,[ab] C. M. Robertson,[a] T. J. Whittles,[bc] Pau Farràs[d] and Alexander J. Cowan*[ab]

A dye-sensitised CO_2 reduction photocatalyst that operates in water is reported. Transient spectroscopy demonstrates that the facile co-immobilisation of a Ru dye and a Ni CO_2 reduction electrocatalyst enables efficient on-particle electron transfer leading to photocatalytic activity that greatly exceeds the equivalent solution based system.

The successful development of materials that can efficiently and cost-effectively enable solar fuel production *via* the reduction of CO_2 and oxidation of water would have a major impact upon the energy landscape. Despite progress in recent years relatively few CO_2 reduction photocatalysts that operate efficiently in water are known.[1–4] Instead many CO_2 reduction photocatalysts are studied in non-aqueous solvents as the increased solubility of CO_2 and decreased proton concentration minimises hydrogen evolution, a competitive reduction reaction which occurs at a similar potential to CO_2 reduction (*e.g.* $CO_2 + 2e^- + 2H^+ \rightarrow CO + H_2O$, $E^0_{SHE} = -0.12$ V).[1]

A promising approach to achieving CO_2 reduction in water is to couple a molecular electrocatalyst to a light absorbing semiconductor or dye molecule that is able to generate sufficiently reducing photoelectrons for transfer to the catalytic centre.[5] This approach has been demonstrated by several groups with a number of studies exploring the coupling of Ru and Re diimine catalysts to a series of different light absorbers including TaON, InP and g-C_3N_4 to achieve visible light driven CO_2 reduction in water.[2,6,7] Ni and Co cyclams (cyclam = 1,4,8,11-tetraazacyclotetradecane) stand out amongst the known electrocatalysts for CO_2 reduction in water as they are highly selective, have relatively low onset potentials and are based only on abundant elements.[8,9] However, to date, attempts to use NiCyc (NiCyc = Ni(cyclam)$^{2+}$) in a photochemical system have demonstrated mixed results. Some studies examined the use of p-type photoelectrodes such as Si, GaP or GaAs with NiCyc in solution; however activity was typically short-lived and a significant (< -0.6 V_{NHE}) applied bias was still required.[10,11] An alternative photocatalytic approach uses $[Ru(bpy)_3]^{2+}$ (bpy = 2,2′-bipyridine) in aqueous solution with NiCyc.[12–15] Here excitation of the ruthenium dye with visible light gives rise to a metal to ligand charge transfer (MLCT) state[16] that is reductively quenched by a sacrificial electron donor, such as ascorbate, to form $[Ru(bpy)_3]^+$ that in turn transfers an electron to NiCyc (Scheme 1a).[13] However initial studies reported low efficiencies, proposed to be due to inefficient electron transfer from the reduced ruthenium dye to NiCyc. Several groups have since developed elegant supramolecular sensitiser/catalyst assemblies[17–19] (Scheme 1b) with the aim of facilitating electron transfer, although to the best of our knowledge none of these systems have shown an increase in activity. This approach also requires the synthesis of complex ligands and linkers which must be redesigned for

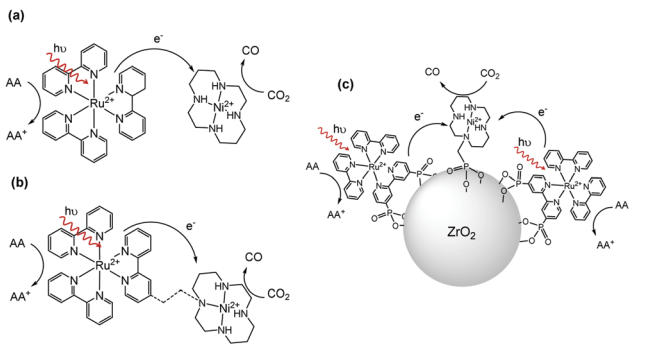

Scheme 1 $[Ru(bpy)_3]^{2+}$ sensitised CO_2 reduction using NiCyc in solution (a) is limited in part by low electron transfer rates. A simple alternative to synthetically complex supramolecular systems (b) is to co-immobilise the catalytic components on a photochemically inert support (c). The dashed line in (b) represents an undefined covalent linkage.

[a] *Department of Chemistry, University of Liverpool, L69 7ZD, UK. E-mail: acowan@liv.ac.uk*
[b] *Stephenson Institute for Renewable Energy, University of Liverpool, L69 7ZD, UK*
[c] *Department of Physics, University of Liverpool, L69 7ZE, Liverpool, UK*
[d] *Department of Chemistry, National University of Ireland Galway, Galway, Ireland*

† Electronic supplementary information (ESI) available: Synthetic procedures, catalyst characterisation and supporting photocatalytic and transient spectroscopic measurements. CCDC 1511267. For ESI and crystallographic data in CIF or other electronic format see DOI: 10.1039/c6cc08590c

each catalyst-sensitiser combination. Co-localization of a chromophore and catalytic centre on a photochemically inert support has been shown to be a facile route to active water splitting materials.[20,21] We hypothesised that such an approach would also be applicable to achieving efficient CO_2 reduction using an immobilised dye and a NiCyc derivative (Scheme 1c), with the close proximity of components enabling efficient on-particle electron transfer.

We previously reported[22] the surface immobilisation of a carboxylic acid functionalised NiCyc on TiO_2; however the catalyst desorbed in water and CO_2. Phosphonate linkages to metal oxide surfaces are known to be more stable in aqueous environments.[23] Therefore CycP (CycP = [(1,4,8,11-tetraaza-cyclotetradecan-1-yl)methylene]phosphonic acid) was synthesised according to literature methods[24] and complexed to $NiCl_2$ to yield the novel catalyst Ni^{II}CycP (synthetic details in ESI,† structure in Fig. 1 inset). Electrochemical studies of NiCycP in solution confirm that the addition of the pendant phosphonate group does not prevent electrocatalytic CO_2 reduction, Fig. 1. Using a hanging mercury drop electrode (HMDE) in 0.1 M $NaClO_4$ (pH 4) with 1 mM NiCycP under argon an irreversible $Ni^{II/I}$ reduction at -1.23 V_{NHE}, similar to the $Ni^{II/I}$ potential of the unsubstituted NiCyc (-1.30 V_{NHE})[8] is observed, Fig. 1a. At potentials negative of -0.95 V_{NHE} a large increase in current for NiCycP occurs under CO_2 due to electrocatalytic CO_2 reduction. The ratio of the peak current in the presence (i_{cat}) and absence (i_p) of CO_2 (i_{cat}/i_p) is a commonly employed measure of catalytic activity and for NiCycP $i_{cat}/i_p = 19$, compared to NiCyc $i_{cat}/i_p = 31$.[22]

NiCycP was immobilised onto ZrO_2 nanoparticles ($\varnothing \sim$ 100–20 nm) by soaking in an ethanolic solution of NiCycP for 48 hours, prior to washing with ethanol to remove unbound NiCycP (details in ESI† 1.2). FTIR and XPS spectroscopies confirm the successful formation of ZrO_2/NiCycP (Fig. S5–S10, ESI†) with binding occurring through the phosphonate linkage. ICP measurements demonstrated that soaking of samples in aqueous solution (pH 4) led to no loss of catalyst into solution confirming the stability of the phosphonate linkage (Table S1, ESI†). Electrochemical studies of ZrO_2/NiCycP on FTO glass were also carried out to confirm that the immobilised catalyst remains electrochemically active, Fig. 1b. In argon-purged CH_3CN with 10% water a cathodic current at potentials negative of -0.8 V_{NHE} (Fig. 1(b)) is observed from an unmodified ZrO_2 electrode in-line with previous studies which have shown the availability of electroactive states at potentials up to 0.5 V below the conduction band edge (*ca.* -1.2 V_{NHE} at pH 4).[25] With a ZrO_2/NiCycP electrode a reduction feature is observed at *ca.* -0.9 V_{NHE} which is assigned to the $Ni^{II/I}$ couple. Under CO_2 the reduction shifts anodically to *ca.* -0.8 V_{NHE}. From these measurements we estimate a driving force for electron transfer from the known phosphonated ruthenium bipyridine dye, RuP (RuP = [Ru^{II}(2,2'-bipyridine)$_2$(2,2'-bipyridine-4,4'-diylbis(phosphonic acid))]) to immobilised NiCycP to be *ca.* -0.3 eV under CO_2 (RuP/RuP^- = -1.1 V_{NHE}).

ZrO_2/RuP/NiCycP photocatalysts were prepared by soaking ZrO_2 nanoparticles in ethanolic solutions of RuP and NiCycP for 48 hours (full details in ESI† 1.2). The presence of both NiCycP and RuP on ZrO_2 was confirmed through FTIR, UV-Vis, ICP and X-ray photoelectron spectroscopies (Fig. S2–S10, ESI†) and quantified by ICP analysis (Table S1, ESI†). Photocatalytic experiments were carried out using 2 mg of ZrO_2/RuP/NiCycP in 2 ml of CO_2-purged ascorbate buffer (pH 4) under illumination (λ = 375–795 nm, 40 mW cm^{-2} incident). As the light-driven reduction of CO_2 to CO is a multi-step process requiring the delivery of two electrons to NiCycP per catalytic cycle, it may be advantageous to have multiple light absorbers per catalytic centre.[26] Therefore we initially screened a number of RuP : NiCycP ratios for CO_2 reduction (Fig. S11, ESI†). This led to the identification of an optimum on particle RuP : NiCycP ratio of *ca.* 2.6 : 1, achieved by the use of a 5 : 1 ([RuP] : [NiCycP], 0.5 mM : 0.1 mM) ethanolic solution. The ability to rapidly screen multiple catalyst and sensitiser ratios highlights an important advantage of the simple on-particle assembly approach.[27] This initial communication focuses on the mechanistic validation of the design approach to CO_2 reduction, however future work will expand this screening study to also explore the optimization of light driven NiCycP systems using scalable visible light sensitisers. For the ZrO_2/RuP/NiCycP (2.6 : 1) photocatalyst we measured photocatalytic CO and H_2 evolution rates of 2.0 ($\pm$0.2) μmol g^{-1} h^{-1} and 8.3 ($\pm$1.3) μmol g^{-1} h^{-1} respectively, normalised for the total mass of the photocatalyst. Considering that the ZrO_2 is an inert support a more appropriate measure of activity may be to only consider the mass of the photo/catalytically active materials (RuP and NiCycP), giving rise to a relatively high CO evolution rate of 322 ($\pm$26) μmol h^{-1} g$^{-1}_{(RuP,\ NicycP)}$ (incident light intensity 40 mW cm^{-2}), Fig. 2. Within 7 hours a turnover number per NiCycP (TON_{Ni}) of 4.8 for CO production was achieved. At prolonged periods activity decreased, presumably due to the reported deactivation pathway of Ni^{I}Cyc-CO formation;[28] however the TON in the on-particle system still greatly exceeds that previously reported for a solution based approach using NiCyc ($TON_{Ni} \sim 0.1$).[13] The achieved selectivity H_2 : CO (4.15 : 1) is relatively low, but it does exceed that originally reported for

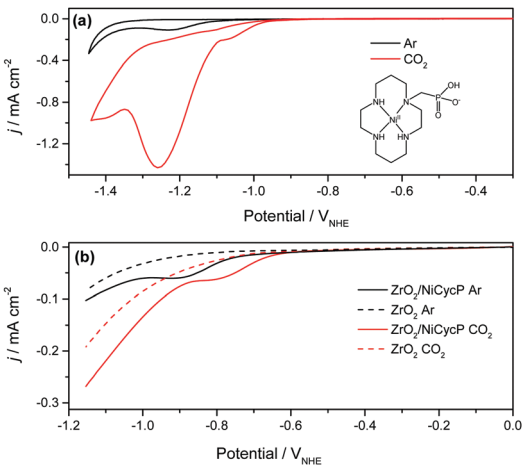

Fig. 1 (a) Cyclic voltammetry of NiCycP in 0.1 M $NaClO_4$ (pH 4) at 100 mV s^{-1} on a HMDE under Ar and CO_2. The structure of NiCycP is shown in the inset. (b) Linear sweep voltammetry of ZrO_2 (dashed lines) and ZrO_2/NiCycP (solid lines) films in CH_3CN/H_2O (9 : 1) 0.1 M $TBAPF_6$ at 100 mV s^{-1} under CO_2 and Ar.

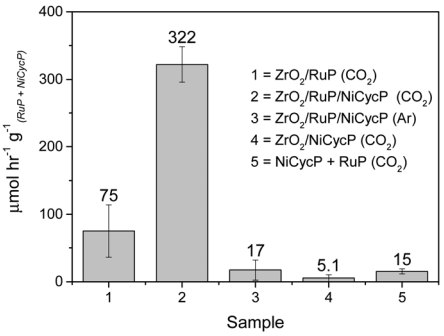

Fig. 2 Rate of photocatalytic CO_2 reduction to CO normalised for the combined mass of RuP and NiCycP in each experiment. In a typical experiment 2 mg of ZrO_2/RuP/NiCycP in 2 ml of CO_2 saturated 0.1 M ascorbate (pH 4) is irradiated with 375–795 nm light, 40 mW cm^{-2} for 7 hours. In experiment 5 a solution of NiCycP (3.4 μM) and RuP (8.9 μM) (0.1 M ascorbate (pH 4)), containing an equivalent Ni and Ru content to experiment 2, was used.

NiCyc in solution at pH 4 (6.4 : 1).[13] To confirm that visible light driven CO_2 reduction is occurring a number of control experiments were carried out, Fig. 2 and Fig. S12–S14 (ESI†). Firstly experiments in the absence of CO_2 (under argon) yielded no significant quantity of CO on the timescales studied, Fig. S13 (ESI†). Isotopic labelling measurements using $^{13}CO_2$ also demonstrated the formation of ^{13}CO, Fig. S12 (ESI†). Experiments in the absence of either the RuP or NiCycP also led to a large loss in activity for CO production, in-line with the proposed mechanism in Scheme 1c being the dominant pathway, Fig. 2. Finally experiments using a 420 long-pass filter showed that CO production is maintained, Fig. S14 (ESI†). Strikingly, control experiments using equivalent quantities of NiCycP (6.8 nmol, 3.4 μM) and RuP (17.8 nmol, 8.9 μM) in a 2 ml 0.1 M ascorbate solution (pH 4, CO_2 purged) showed a ×30 decrease in activity compared to the equivalent ZrO_2/RuP/NiCycP sample (Fig. 2) with a TON_{Ni} = 0.16 for CO production after 7 hours. It is therefore apparent that the activity of the on-particle system greatly exceeds the equivalent solution based system.

For the remainder of the communication we have used transient absorption (TA) and time resolved photoluminescence (TR-PL) spectroscopy to explore the hypothesis that the enhanced photocatalytic activity for the on-particle is due to improved electron transfer from photogenerated RuP^- to NiCycP, Scheme 2. Steady state emission spectroscopy of RuP/ZrO_2 films excited at 435 nm

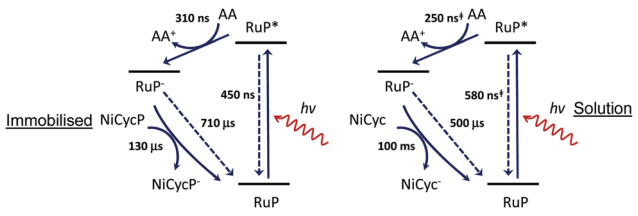

Scheme 2 Kinetic scheme for the light driven reduction of NiCycP leading to CO_2 reduction using on particle ZrO_2/RuP/NiCycP compared to the dye and catalyst in solution. Lifetimes of exponential fits from TA and emission studies are given in bold. ‡ Values taken from ref. 21.

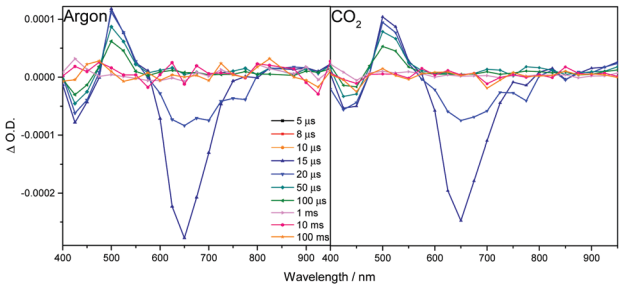

Fig. 3 TA spectra of ZrO_2/RuP/NiCycP in the presence of 0.1 M ascorbate (pH = 4) under argon and under CO_2, following 355 nm (6 ns) excitation at the time delays indicated. Both spectra show the presence of a transient feature centred at *ca.* 510 nm assigned to RuP^-.

showed the formation of the MLCT excited state (RuP*, λ_{em} = 618 nm)[16] which was partially quenched in the presence of 0.1 M ascorbate (pH 4), Fig. S18 (ESI†). In line with past reports we measured a quenching lifetime of *ca.* 310 ns by TR-PL, Fig. S17 (ESI†).[21] TA spectroscopy of ZrO_2/RuP in water (pH 4) following 355 nm excitation showed the formation of a ground state bleach (400–500 nm) and an excited state absorption feature *ca.* 625 nm that was heavily overlapped with the large negative feature from 550 nm to 750 nm due to the strong emission of RuP* (Fig. S15a, ESI†).[23] In-line with past reports we see no evidence for the formation of RuP^+ (λ_{max} = 700 nm) confirming that electron injection into ZrO_2 cannot occur from the dye excited state (RuP^+/RuP* = −0.95 V_{NHE}).[29] TA spectra of ZrO_2/RuP (Fig. S15b, ESI†) and ZrO_2/RuP/NiCycP (Fig. 3a) in 0.1 M ascorbate solution both showed similar features with a bleach at 425 nm, corresponding to the loss of the ground state, and a positive absorption at *ca.* 510 nm that can be readily assigned to RuP^- [21] overlapped with a broad negative feature (λ_{max} *ca.* 650 nm) due to the remaining emission from the MLCT excited state. TA spectroscopy therefore confirms that reductive quenching of a fraction of the RuP* population by ascorbate is occurring. The decay of the 510 nm feature of ZrO_2/RuP^- is well fitted to a single stretched exponential function of the form $\Delta OD_{510nm} = y_0 + A_1 e^{(-kt)^\beta}$ with an apparent first order rate constant $k_{app} = 1.4 \times 10^3\ s^{-1}$ (Fig. 4a, see ESI† Section 3 for the full kinetic model). It has been shown that electron

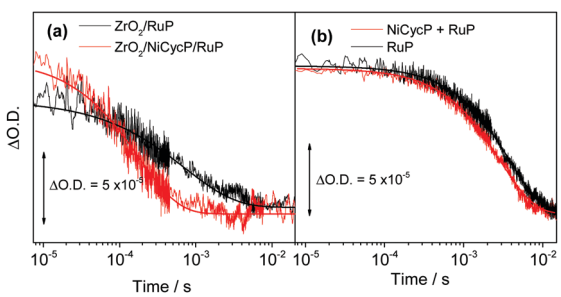

Fig. 4 (a) TA kinetic traces of RuP^- (510 nm) showing the accelerated decay of RuP^- for ZrO_2/RuP/NiCycP in 0.1 M ascorbate following 355 nm (6 ns) excitation. (b) Kinetic trace of RuP^- in solution following the 355 nm excitation of RuP (8.9 μM) in 0.1 M ascorbate in the presence and absence of NiCycP (60 μM). The kinetic traces are fitted to (a) stretched exponential and (b) mono-exponential decays.

injection[21] into the ZrO_2 conduction band does not occur from RuP^- therefore it is proposed that the loss of RuP^- in ZrO_2/RuP is primarily due to the back reaction with oxidised ascorbate species.[17] Significantly we find that the rate of RuP^- decay is greatly accelerated with ZrO_2/RuP/NiCycP (k_{app} = 7.8 × 10^3 s^{-1}). Under CO_2 no change in the rate of electron transfer to NiCycP was observed (Fig. 3b). The weak extinction coefficient of NiCyc and its related complexes (*e.g.* NiCycP in solution (aq), λ_{max} = 344 nm (24 $M^{-1}cm^{-1}$) and 533 nm (12 $M^{-1}cm^{-1}$)), coupled to the spectral range of our TA instrument (λ_{probe} 450–950 nm), prevents direct observation of the formation of $NiCycP^-$ (*ca.* 390 nm).[17] Nonetheless the accelerated rate of decay of RuP^- upon co-immobilisation of NiCycP strongly indicates that efficient electron transfer can occur from RuP^- to NiCycP, in line with the calculated driving force for this process (*ca.* −0.3 eV).

A simple kinetic analysis based on 2 parallel decay pathways for RuP^- in solution, namely forward electron transfer from RuP^- to NiCyc which is in competition with back electron between RuP^- and oxidised ascorbate, has been reported elsewhere.[17] Here we apply the same model to calculate an electron transfer yield on the order of 82% for the reduction of NiCycP by photogenerated RuP^- on ZrO_2/RuP/NiCycP, see ESI† Section 3 for details. Experiments carried out using RuP (8.9 μM) in 0.1 M ascorbate (pH 4) solution also show the rapid formation of RuP^-, observed by TA spectroscopy at 510 nm; however in contrast to the immobilised system in solution the addition of NiCycP only slightly decreases the lifetime of RuP^- even at very high NiCycP concentrations (60 μM), Fig. 4b. Using the reagent concentrations employed for the solution photocatalysis experiments described above (8.9 μM RuP, 3.4 μM NiCycP) we find k_{app} = 1.9 × 10^2 s^{-1}, leading to an estimated electron transfer yield from RuP^- to NiCycP in solution of only *ca.* 5% indicating that the back reaction with oxidised ascorbate dominates, in line with the greatly decreased photocatalytic activity observed. Whilst the consideration of only 2 decay pathways for RuP^- is a simplified model, during photocatalysis a range of alternative decay pathways are likely to become accessible as catalytic intermediates and oxidised scavengers accumulate, it does nonetheless clearly demonstrate that co-localisation of the dye and catalyst is sufficient for efficient charge transfer.

Co-immobilisation of a catalytic centre and visible light absorber onto a photochemically inert support offers a facile route to developing photocatalytic materials for CO_2 reduction that is likely to be applicable to a large number of combinations of existing dyes and CO_2 reduction electrocatalysts. Such an approach has been widely applied to photocatalytic water splitting[20,21,27] and here we explore a model CO_2 reduction system that operates in water. The focus of this communication has been on demonstrating the efficiency of the on-particle electron transfer pathway. Significantly we demonstrate that efficient on-particle electron transfer can occur, thus avoiding the need to develop complex supramolecular dye-catalyst complexes. The on-particle electron transfer pathway also offers a simple alternative to current state-of-the-art through particle dye-sensitised CO_2 reduction systems[30,31] that have been demonstrated in organic solvents to be highly sensitive to the presence of ionic additives. This communication also represents a significant improvement in the reported activity for light-driven CO_2 reduction by NiCyc, and ZrO_2/RuP/NiCycP is one of only a relatively small number of water active CO_2 reduction photocatalysts. Currently our selectivity towards CO_2 is relatively low, despite NiCyc being known to be a highly selective electrocatalyst. This may be in part due to the use of RuP in aqueous solutions (Fig. S19, ESI†) or the choice of electron donor and screening studies are now underway to explore alternative electron donors and lower cost sensitisers and these will be reported shortly.

The EPSRC is acknowledged for a fellowship (EP/K006851/1) supporting AJC and JJW and for equipment (EP/K031511/1) and a studentship (EP/J500471/1) for TJW. PF thanks the Royal Society for funding. The authors thank Dr V. Dhanak for XPS access.

Notes and references

1 W. Tu, Y. Zhou and Z. Zou, *Adv. Mater.*, 2014, **26**, 4607–4626.
2 A. Nakada, T. Nakashima, K. Sekizawa, K. Maeda and O. Ishitani, *Chem. Sci.*, 2016, **7**, 4364–4371.
3 A. Nakada, K. Koike, T. Nakashima, T. Morimoto and O. Ishitani, *Inorg. Chem.*, 2015, **54**, 1800–1807.
4 D. J. Boston, C. Xu, D. W. Armstrong and F. M. MacDonnell, *J. Am. Chem. Soc.*, 2013, **135**, 16252–16255.
5 H. Tian, *ChemSusChem*, 2015, **8**, 3746–3759.
6 T. Arai, S. Sato, T. Kajino and T. Morikawa, *Energy Environ. Sci.*, 2013, **6**, 1274–1282.
7 R. Kuriki, H. Matsunaga, T. Nakashima, K. Wada, A. Yamakata, O. Ishitani and K. Maeda, *J. Am. Chem. Soc.*, 2016, **138**, 5159–5170.
8 M. Beley, J.-P. Collin, R. Ruppert and J.-P. Sauvage, *J. Chem. Soc., Chem. Commun.*, 1984, 1315–1316.
9 G. Neri, I. M. Aldous, J. J. Walsh, L. J. Hardwick and A. J. Cowan, *Chem. Sci.*, 2016, **7**, 1521–1526.
10 J. P. Petit, P. Chartier, M. Beley and J. P. Deville, *J. Electroanal. Chem.*, 1989, **269**, 267–281.
11 M. G. Bradley, T. Tysak, D. J. Graves and N. A. Viachiopoulos, *J. Chem. Soc., Chem. Commun.*, 1983, 349.
12 C. A. Craig, L. Spreer, J. W. Otvos and M. Calvin, *J. Phys. Chem.*, 1990, **94**, 7957–7960.
13 J. L. Grant, K. Goswami, L. O. Spreer, J. W. Otvos and M. Calvin, *J. Chem. Soc., Dalton Trans.*, 1987, 2105.
14 M. A. Méndez, P. Voyame and H. H. Girault, *Angew. Chem., Int. Ed.*, 2011, **50**, 7391–7394.
15 S. Montanaro, C. Herrero, D. Merli, M. Fagnoni, A. Poggi, S. Protti, S. Sheth and A. Albini, *Green Process Synth.*, 2013, **2**, 335–343.
16 D. W. Thompson, A. Ito and T. J. Meyer, *Pure Appl. Chem.*, 2013, **85**, 1257–1305.
17 C. Herrero, A. Quaranta, S. El Ghachtouli, B. Vauzeilles, W. Leibl and A. Aukauloo, *Phys. Chem. Chem. Phys.*, 2014, **16**, 12067.
18 E. Kimura, X. Bu, M. Shionoya, S. Wada and S. Maruyama, *Inorg. Chem.*, 1992, **31**, 4542–4546.
19 E. Kimura, S. Wada, M. Shionoya and Y. Okazaki, *Inorg. Chem.*, 1994, **33**, 770–778.
20 M. Hansen, F. Li, L. Sun and B. König, *Chem. Sci.*, 2014, **5**, 2683–2687.
21 M. A. Gross, A. Reynal, J. R. Durrant and E. Reisner, *J. Am. Chem. Soc.*, 2014, **136**, 356–366.
22 G. Neri, J. J. Walsh, C. Wilson, A. Reynal, J. Y. C. Lim, X. Li, A. J. P. White, N. J. Long, J. R. Durrant and A. J. Cowan, *Phys. Chem. Chem. Phys.*, 2014, **17**, 1562–1566.
23 J. Willkomm, K. L. Orchard, A. Reynal, E. Pastor, J. R. Durrant and E. Reisner, *Chem. Soc. Rev.*, 2016, **45**, 9–23.
24 S. Füzerová, J. Kotek, I. Císařová, P. Hermann, K. Binnemans and I. Lukeš, *Dalton Trans.*, 2005, 2908–2915.
25 B. I. Lemon, F. Liu and J. T. Hupp, *Coord. Chem. Rev.*, 2004, **248**, 1225–1230.
26 A. J. Cowan and J. R. Durrant, *Chem. Soc. Rev.*, 2013, **42**, 2281–2293.
27 A. Králík, M. Hansen and B. König, *RSC Adv.*, 2016, **6**, 5739–5744.
28 G. B. Balazs and F. C. Anson, *J. Electroanal. Chem.*, 1993, **361**, 149–157.
29 H. Park, E. Bae, J. J. Lee, J. Park and W. Choi, *J. Phys. Chem. B*, 2006, **110**, 8740–8749.
30 E.-G. Ha, J.-A. Chang, S.-M. Byun, C. Pac, D.-M. Jang, J. Park and S. O. Kang, *Chem. Commun.*, 2014, **50**, 4462.
31 D.-I. Won, J.-S. Lee, J.-M. Ji, W.-J. Jung, H.-J. Son, C. Pac and S. O. Kang, *J. Am. Chem. Soc.*, 2015, **137**, 13679–13690.